

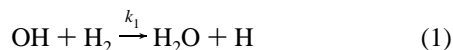
Kinetics of Hydroxyl Radical Reactions with Isotopically Labeled Hydrogen

Ranjit K. Talukdar,[†] Tomasz Gierczak,^{†,‡} Leah Goldfarb,[§] Yinon Rudich,^{||}
B. S. Madhava Rao,[⊥] and A. R. Ravishankara^{*,§}National Oceanic and Atmospheric Administration, Aeronomy Laboratory, 325 Broadway,
Boulder, Colorado 80303Received: July 7, 1995; In Final Form: November 7, 1995[⊗]

The rate coefficients for the reactions of hydroxyl radical (OH) with H₂ (k_1), HD (k_2), and D₂ (k_3) were measured between ~230 and ~420 K to be $k_1 = 7.21 \times 10^{-20} T^{2.69} \exp(-1150/T)$, $k_2 = 5.57 \times 10^{-20} T^{2.7} \exp(-1258/T)$, and $k_3 = 5.7 \times 10^{-20} T^{2.73} \exp(-1580/T)$ cm³ molecule⁻¹ s⁻¹ using pulsed photolysis to generate OH and laser-induced fluorescence to detect it. Using the same method, the rate coefficients for the reactions of OD with H₂ and D₂ were measured to be equal to k_1 and k_3 , respectively. In reaction 2, the yield of H was measured to be 0.17 ± 0.03 and 0.26 ± 0.05 at 250 and 298 K, respectively, by detecting it using CW Lyman- α resonance fluorescence. k_2 was found to be half the sum of k_1 and k_3 over the entire temperature range of this study. The quoted uncertainties are at the 95% confidence level and include estimated systematic errors. On the basis of these findings it is suggested that most, if not all, of the reaction in the range of temperatures studied here may be occurring via tunneling of H/D atoms through the barrier.

Introduction

The reaction of OH with H₂,



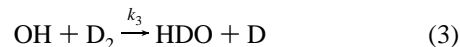
plays a significant role in atmospheric chemistry because of the large abundance, ~0.5 ppmv, of H₂ in Earth's atmosphere. It is a significant contributor to the conversion of OH to HO₂ in the troposphere. H₂ is produced, at least in part, from the oxidation of methane and non-methane hydrocarbons and is primarily removed via reaction 1. Since the isotopic abundance of D in hydrogen is related to that in methane, knowledge of the atmospheric flux of H₂ and HD will help elucidate the sources of CH₄. The flux calculation requires the rate of removal of HD, which is also expected to be controlled by OH reaction. Therefore, the rate coefficients for the reaction



are needed.

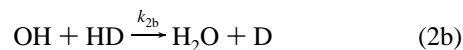
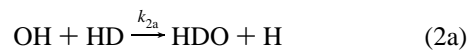
Reaction 1 is a key reaction in the combustion of H₂. Therefore, there are numerous measurements of k_1 as a function of temperature up to ~3000 K.¹ Because the reaction of hydroxyl radicals with hydrogen is one of the simpler radical-molecule reactions, it is amenable to theoretical investigations. The potential energy surfaces (PES's) for the reaction of hydroxyl radical with hydrogen have been computed,²⁻⁵ and the rate coefficients have been calculated using these surfaces.^{1,5-7} The accuracy of the PES and the calculated rate constants can be evaluated by varying the isotopic composition of the

reactants. Therefore, in addition to reactions 1 and 2, the rate coefficient for the reaction



was measured to provide a consistent set of low-temperature rate coefficients for comparison with calculations.

Reaction 2 has an added feature in that it can lead to distinguishable products, H and HDO (reaction 2a) or D and H₂O (reaction 2b),



The product yields in reaction 2 should also be calculable from the *ab initio* PES. We have measured the branching ratio for H atom production in reaction 2 to provide experimental data for comparison with calculations.

Isotopic substitution of the hydroxyl radical, i.e., OH vs OD, should not significantly alter the rate coefficient for the hydroxyl radical reaction with hydrogen because such a substitution involves a secondary kinetic isotope effect. To estimate the secondary kinetic isotope effect, we have also studied the reactions



Experiments and Results

During this study, k_1 – k_5 were measured by observing the temporal profiles of OH/OD detected via pulsed laser induced fluorescence (LIF) in known concentrations of H₂, D₂, or HD. The branching ratio in reaction 2, k_{2a}/k_2 , was measured by detecting H atoms via CW Lyman- α resonance fluorescence. The apparatus and the data acquisition/analysis methodology for such measurements have been used extensively and are described elsewhere.⁸⁻¹² The major difference between the current and previous methodology was the use of a circulation

* Address correspondence to this author at: NOAA/ERL, R/E/AL2, 325 Broadway, Boulder, CO 80303.

[†] Also associated with the Cooperative Institute for Research in Environmental Sciences, University of Colorado, Boulder, CO.

[‡] Permanent address: Department of Chemistry, Warsaw University, ul. Zwirki i Wigury 101, 02-089, Warszawa, Poland.

[§] Also associated with the Department of Chemistry and Biochemistry, University of Colorado, Boulder, CO 80309.

^{||} NOAA/NRC postdoctoral research associate.

[⊥] Permanent address: Department of Chemistry, University of Pune, Pune 411 007, India.

[⊗] Abstract published in *Advance ACS Abstracts*, January 15, 1996.

system to minimize the use of expensive HD in some experiments. k_1 and k_2 were also determined while measuring the yield of H atoms in reaction 2 by monitoring H atom temporal profiles.

Materials and Sample Handling. Samples of H₂, HD, and D₂ were analyzed for the presence of impurities using a gas chromatograph (GC) equipped with capillary columns (DB-5 and GS-AL columns from J & W Scientific) and a flame ionization detector. H₂ was obtained from Scott Specialty Gases (99.99%) and contained <1 ppmv of hydrocarbons. D₂, obtained from Matheson Gas Products with an isotopic purity of 99.9%, contained less than 0.5 ppmv of impurity, which was mostly ethane. HD, obtained from Cambridge Isotope Laboratories, had an isotopic purity of 97% and contained an unknown impurity which condensed at liquid N₂ temperature. This HD sample was transferred to a 5 L Pyrex bulb which was connected through a Teflon stopcock to a cold finger maintained at liquid N₂ temperature. After 15 h of exposure to the cold finger, the HD sample was withdrawn and was found to contain <10 ppmv of small saturated hydrocarbons, presumably methane and ethane. As shown later, these impurities did not lead to significant errors in the measured rate coefficients.

The closed-loop circulation system employed in measuring k_2 was equipped with a ~3-L ballast volume, a Teflon circulation pump, throttle valves, and inlets in tandem with the reactor. Water was used as the photolyte because it is a stable compound, does not isotope exchange with HD at the temperatures of this study, and photolyzes at wavelengths where hydrogen does not absorb. The concentrations of HD in the circulating mixtures were determined from the known pressure, concentration of the premade mixtures, and dilution factors. As a test of the reliability of the circulation system, the rate coefficient for the OH + CH₄ reaction was measured at 298 K and found to be in excellent agreement with the recommended value.^{13,14} Further, k_1 measured using the circulation system was the same as that obtained in the conventional flow system. Lastly, the value of k_2 measured at 298 K using the conventional pump-out configuration was the same as that determined using the circulation system.

After exposure to air, there were often reactive impurities on the inside surfaces of the circulation system that enhanced the decay rate of OH. To remove these impurities, at the beginning of an experiment, a gas mixture containing H₂O was circulated through the system while the photolysis lamp was pulsing. The OH decay rates measured after this procedure did not change with time. To make sure that the gases were well mixed, each gas mixture was circulated in the system for approximately 15 min before acquiring kinetic data. During the course of determining k_2 , many pseudo-first-order rate coefficients were remeasured using the same concentrations of HD; the obtained values of k_2 did not change. The reaction mixture circulating through the system was subjected to many photolysis pulses and then analyzed by GC. No new impurities were detected. It is worth noting that photolysis of a mixture of hydrogen and water does not change the composition. It is possible that small amounts of H₂O₂ were produced; however, H₂O₂ was not a significant stable product, since the measured decay rates of OH did not change with photolysis duration. Also, there was no significant buildup of O₂, which would have led to OH regeneration at long times via the formation of HO₂ and its subsequent reaction with H/D atoms.

OH/OD Kinetics. The OH (OD) radicals were generated by one or more of the following methods: (1) photolysis of H₂O (D₂O) by a Xe flash lamp (165 nm < λ < 185 nm), (2) photolysis of H₂O₂ (D₂O₂) at 248 nm (KrF laser) or at 193 nm

TABLE 1: Values of k_1 , k_2 , and k_3 (in Units of 10⁻¹⁵ cm³ molecule⁻¹ s⁻¹) Measured by Monitoring the Temporal Profile of OH^a

<i>T</i> , K	$k_1 \pm 2\sigma^b$	<i>T</i> , K	$k_2 \pm 2\sigma^c$	<i>T</i> , K	$k_3 \pm 2\sigma^d$
238	1.46 ± 0.04	248	1.07 ± 0.04 ^f	242	0.265 ± 0.020 ^g
252	2.09 ± 0.12	258	1.38 ± 0.04 ^f	242	0.331 ± 0.015
267	3.10 ± 0.10	263	1.57 ± 0.14	242	0.332 ± 0.02
297	6.50 ± 0.13	268	1.79 ± 0.03 ^f	243	0.316 ± 0.024
323	11.8 ± 0.50	273	1.99 ± 0.09	243	0.251 ± 0.037
348	18.0 ± 0.20	286	2.78 ± 0.14	254	0.428 ± 0.03
373	27.3 ± 0.60	298	3.94 ± 0.26	258	0.484 ± 0.04 ^g
400	40.3 ± 0.70	313	5.16 ± 0.28 ^f	263	0.59 ± 0.03
		315	6.14 ± 0.18	268	0.66 ± 0.04
		323	6.48 ± 0.42	285	1.08 ± 0.04
	PP-RF	337	9.35 ± 0.18	297	1.69 ± 0.10 ^e
245	2.05 ± 0.20	355	11.92 ± 0.68	298	1.57 ± 0.04 ^d
263	2.85 ± 0.45	373	16.18 ± 0.12	299	1.72 ± 0.10 ^g
273	3.8 ± 0.2	398	24.53 ± 0.40	301	1.80 ± 0.07
300	7.4 ± 2.1	418	29.38 ± 1.52 ^f	315	2.12 ± 0.15
323	10 ± 1			334	3.29 ± 0.15
348	16 ± 2		PP-RF	363	6.85 ± 0.16
373	23 ± 7	298	5 ± 1	401	14.1 ± 0.16

^a Rate coefficients measured by following H atom growth are listed under PP-RF. The error bar includes 2 σ precision only. The pressure in the reaction cell was 100 Torr for most experiments and 300 Torr in a few cases. ^b Photolysis of H₂O₂ at 248 nm was used as the OH source except where noted. ^c Photolysis of H₂O by Xe flash lamp (165–185 nm) was used as the only OH source. ^d Photolysis of N₂O at 193 nm to generate O(¹D) followed by reaction with H₂O/D₂O to produce OH/OD except where noted. ^e Photolysis of H₂O₂ at 193 nm was used to generate OH. ^f The flash lamp energy was 1/4 of the maximum energy. ^g Photolysis of H₂O₂ at 248 nm.

(ArF laser), or (3) photolysis of N₂O at 193 nm (ArF laser) to generate O(¹D), which reacted with H₂O (D₂O). OH and OD were detected by pulsed LIF as described elsewhere.⁹ The detection limit for OH was 1 × 10⁸ cm⁻³ for integrating 100 laser shots in the presence of 3 × 10¹⁶ cm⁻³ of H₂O and 100 Torr of He. The detection limit for OD was similar to that for OH.

Reactions 1–5 are highly temperature sensitive. Therefore, the temperature of the gas mixture in the reaction zone, defined by the intersection of the photolysis and probe laser beams, was directly measured by a shielded thermocouple prior to and after the acquisition of a rate coefficient and was estimated to be accurate to ±0.5 K.

All experiments were carried out under pseudo-first-order conditions in OH or OD. The initial concentrations of OH and OD were <3 × 10¹¹ cm⁻³, while concentrations of H₂, HD, or D₂ were 10⁵–10⁶ times larger. Therefore, the temporal profiles of [OH] or [OD] followed the equation

$$\frac{d \ln S}{dt} = -k_i[X_i] + k_b = -k' \quad (I)$$

where $i = 1-5$, X_i refers to H₂/HD/D₂ (as appropriate) in reaction i , $k' = k_i[X_i] + k_b$, S is the LIF signal from OH or OD, and k_b is the first-order rate coefficient for the loss of OH/OD in the absence of the reactant. The concentration of the photolyte (H₂O, H₂O₂, or N₂O) and the photolysis energy were held constant during the course of measuring a particular bimolecular rate constant. Keeping the concentration of H₂O₂ constant was particularly important because it reacts with OH and contributes to the measured value of k_b ; if [H₂O₂] changed, k_b would change. Weighted (according to the signal to noise) least squares fits of the LIF signals at various reaction times to eq I yielded k' . The second-order rate coefficients, k_1 – k_5 , were obtained from weighted linear least squares analyses of the measured values of k' at various concentrations of H₂, HD, and D₂. Results of such measurements, repeated at different temperatures, are listed in Table 1.

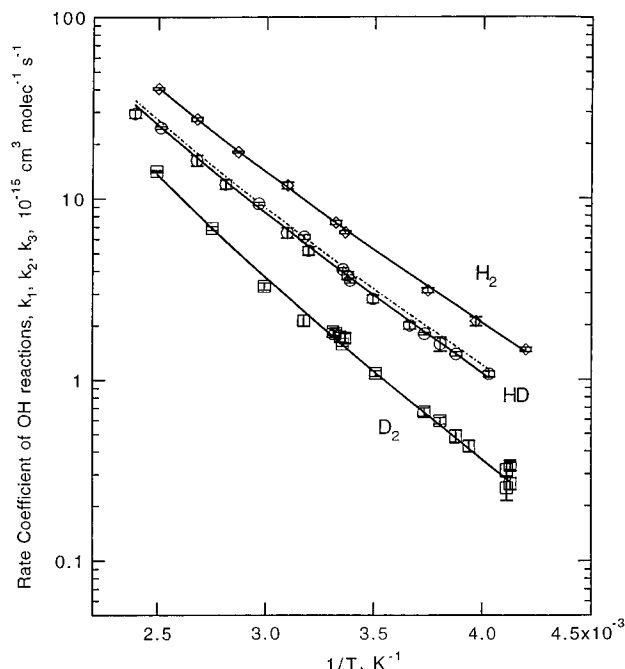


Figure 1. Plot of the second-order rate coefficients, k_1 , k_2 , and k_3 , on a logarithmic scale, as a function of $1/T$. The solid lines are the fit of the data to a three-parameter modified Arrhenius form ($k_i = AT^n e^{-E/RT}$). The dashed line traced along the HD data (k_2) is the average of k_1 and k_3 , i.e., $k_2 = (k_1 + k_3)/2$.

All OH kinetic studies (including those using the circulator) were carried out under a slow steady flow of the gas mixture. The linear gas flow velocity in the reaction zone was ~ 5 – 15 cm s^{-1} . The total pressure in the reactor was usually in the range 50–300 Torr. Experimental conditions, such as $[\text{OH}]_0$, total pressure, lamp energy, and linear gas flow rates were varied to check for possible errors due to secondary reactions; no dependence on any of these variables was observed.

The measured values of k_1 – k_3 are plotted as a function of $1/T$ in Figure 1. They were fitted to the conventional Arrhenius form, $k = Ae^{-E/RT}$, as well as to a three-parameter form, $k = AT^n e^{-E/RT}$. The obtained values of A , E/R , and n are listed in Table 2 along with $k(298 \text{ K})$. The quoted uncertainties in the values of A and E/R from this study are at the 95% confidence limit. The uncertainties in the E/R values presented in the format adapted by NASA/JPL¹³ and IUPAC/CODATA¹⁴ evaluations were chosen to represent the uncertainties in the values of the rate constants at temperatures not equal to 298 K.

Also shown in Table 2 are the rate coefficients for the reactions of OD with H_2 (k_4) and D_2 (k_5). The value of k_4 measured at 302 K was $(7.4 \pm 0.4) \times 10^{-15} \text{ cm}^3 \text{ molecule}^{-1} \text{ s}^{-1}$, which leads to $k_4(298 \text{ K}) = (6.8 \pm 0.4) \times 10^{-15} \text{ cm}^3 \text{ molecule}^{-1} \text{ s}^{-1}$ by assuming that the E/R value for k_4 is the same as that for k_1 . The measured value of k_5 at 302 K was $(1.84 \pm 0.13) \times 10^{-15} \text{ cm}^3 \text{ molecule}^{-1} \text{ s}^{-1}$, which translates to $k_5(298 \text{ K}) = (1.65 \pm 0.13) \times 10^{-15} \text{ cm}^3 \text{ molecule}^{-1} \text{ s}^{-1}$ by

TABLE 2: Comparison of Measured k_1 – k_5 with Those from Previous Works^a

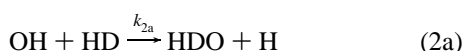
$k(298 \text{ K})^b$	A	n	$E/R \pm \Delta E/R$ (K)	T range (K)	comment ^c	ref
OH + H_2 (k_1)						
6.7 ± 1.5	7.7		2100 ± 200	200–450		14
6.7 ± 1.2	5.5		2000 ± 400	200–300		13
6.65 ± 0.36^d	5.44 ± 0.27	2.69	1983 ± 17	238–400	PP–LIF	this work
	7.21×10^{-8}		1150	238–400	PP–LIF	this work
6.65	5.4		2000 ± 25	238–400	$f(298 \text{ K}) = 1.08$	this work rec ^e
OH + HD (k_2)						
3.95 ± 0.12					relative	32
3.96 ± 0.32^d	4.98 ± 0.32	2.7	2121 ± 21	248–418	FP–LIF	this work
	5.57×10^{-8}		1258	248–418	FP–LIF	this work
3.96	5.00		2130 ± 25	248–418	$f(298 \text{ K}) = 1.08$	this work rec ^e
OH + D_2 (k_3)						
2.1 ± 0.18					FP–RA	30
2.05 ± 0.31					VUV FP–RF	39
1.99 ± 0.26^f					FP–RA	40
1.83 ± 0.12	12.1 ± 5.2	1.18	2671 ± 147	250–470	FP–RF	24
	4.37×10^{-3}		2332	250–1050	FP–RF	24
2.2 ± 0.4	$12.5^{+6.0}_{-4.0}$		2587 ± 181	210–460	FP–RF	29
1.64 ± 0.13^d	6.21 ± 0.33	3.47	2456 ± 19	242–401	PP–LIF	this work
	3.43×10^{-10}		1324	242–401	PP–LIF	this work
	5.64 ± 0.27		2420 ± 16	242–401		ref 24
	5.7×10^{-8}	2.73	1580			+ this work
1.64	6.21		2456 ± 20	242–401	$f(298 \text{ K}) = 1.08$	this work rec ^e
OD + H_2 (k_4)						
6.8 ± 0.40^f						this work
OD + D_2 (k_5)						
1.88 ± 0.30					PP–LIF	31
2.21 ± 0.22					FP–RA	30
1.65 ± 0.13^f					PP–LIF	this work

^a Our quoted error bars are at the 95% confidence level and include estimated systematic errors. k and A are in the units of 10^{-15} and $10^{-12} \text{ cm}^3 \text{ molecule}^{-1} \text{ s}^{-1}$, respectively. ^b The 298 K values quoted here were obtained from an average of $k(298 \text{ K})$ calculated from the Arrhenius expression and the measured values of k at T in the range $295 \leq T \leq 300 \text{ K}$. Data close to 298 K were normalized to 298 K using E/R measured here. ^c FP–LIF: Flash photolysis (H_2O using Xe flash lamp)–laser-induced fluorescence detection of OH. PP–LIF: Pulsed (laser) photolysis–laser-induced fluorescence detection of OH. FP–RF: Flash photolysis–resonance fluorescence detection of OH. FP–RA: Flash photolysis–resonance absorption detection of OH. ^d Includes estimated systematic error of 5% in concentrations of H_2 , HD, and D_2 . ^e These are our values in the format used in NASA and IUPAC/CODATA recommendations. Uncertainty at temperature T is given by $f(T) = f(298 \text{ K}) \exp\{(\Delta E/R)((1/T) - (1/298))\}$. ^f This value was obtained by transforming the measured data at temperatures other than room temperature by using activation energy E/R for reactions 1 and 3 determined in this work.

assuming $E/R = 2460$ K. The quoted error bars include an estimated 5% uncertainty in concentrations of D_2 and H_2 .

H Atom Kinetics. The yield of H atoms in the reaction of OH with HD (reaction 2) was measured relative to that in reaction 1. They were placed on an absolute scale by assuming the H atom yield in reaction 1 to be unity. The Lyman- α lines of H and D atoms are very close to each other. D atoms are produced in reaction 2b. If D atoms are detected by the H atom lamp, the measured temporal profiles cannot be attributed to only H atoms. Therefore, we checked to see if D atoms were detected by the H atom detection system by generating only D atoms via the $O(^1D) + D_2$ reaction; D atoms were not detected.

OH radicals ($< 1 \times 10^{12} \text{ cm}^{-3}$) were produced via 248 nm photolysis of H_2O_2 ($\sim 5 \times 10^{14} \text{ cm}^{-3}$) or of ozone ($2-5 \times 10^{12} \text{ cm}^{-3}$); $O(^1D)$ from O_3 photolysis reacted with H_2 to make OH or with HD to make OH and OD. The concentration of H_2 and HD were in the range $(2-20) \times 10^{17} \text{ cm}^{-3}$. Postphotolysis reactions are illustrated for the H_2O_2 source and HD reactant:



The temporal profile of H atoms is given by

$$[H]_t = (\alpha \times e^{-\beta t}) - (\gamma \times e^{-\delta t}) \quad (II)$$

where

$$\alpha_{HD} = \{k_{2a}[OH]_0[HD]\} / \{k_7[H_2O_2] + k_2[HD] + k_{OH} - k_H\} = \gamma_{HD} \quad (IIIa)$$

$$\beta_{HD} = k_H \quad (IIIb)$$

and

$$\delta_{HD} = \{k_7[H_2O_2] + k_2[HD] + k_{OH}\} \quad (IIIc)$$

The $H + HD \rightarrow H_2 + D$ ($k(298 \text{ K}) = 4.5 \times 10^{-17} \text{ cm}^3 \text{ molecule}^{-1} \text{ s}^{-1}$) and $D + HD \rightarrow D_2 + H$ ($k(298 \text{ K}) = 4.3 \times 10^{-17} \text{ cm}^3 \text{ molecule}^{-1} \text{ s}^{-1}$) reactions are too slow at the temperatures used in our measurements to cause any interference. Therefore, these reactions were not included in deriving the above rate expression. Rate coefficients for the $H + HD$ and $D + HD$ reactions were estimated from the experimentally determined rate constants of the reverse reactions, $D + H_2$ and $H + D_2$,^{15,16} and the known thermodynamic quantities.¹⁷ In the presence of H_2 , the parameters in eq II are given by

$$\alpha_{H_2} = \{k_1[OH]_0[H_2]\} / \{k_7[H_2O_2] + k_1[H_2] + k_{OH} - k_H\} = \gamma_{H_2} \quad (IVa)$$

$$\beta_{H_2} = k_H \quad (IVb)$$

and

$$\delta_{H_2} = \{k_7[H_2O_2] + k_1[H_2] + k_{OH}\} \quad (IVc)$$

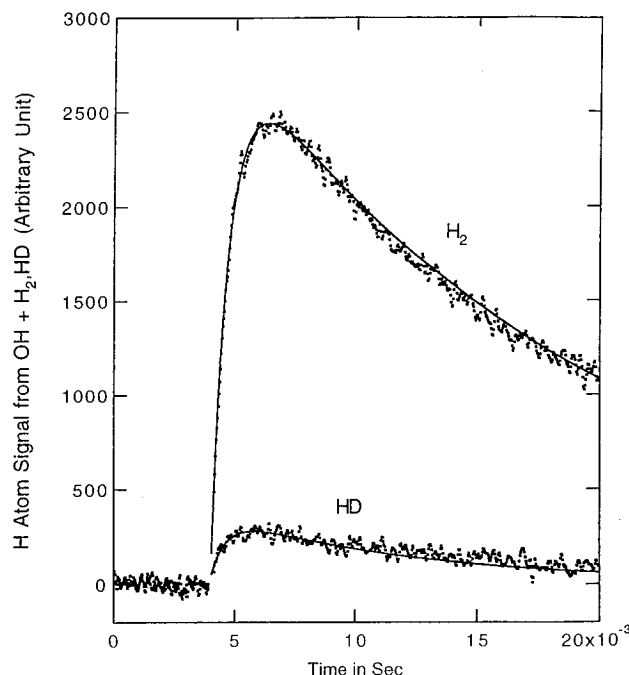


Figure 2. H atom temporal profiles in the reactions of OH with HD and H_2 at 250 K and 60 Torr pressure. The concentrations of H_2 and HD were 5.6×10^{17} and $5.3 \times 10^{17} \text{ molecule cm}^{-3}$, respectively. The solid lines are the biexponential fits to eq II (see text for details). The rate coefficients, k_1 and k_2 , and the yields of H atom in reaction 2a were determined from the fitted parameters.

The parameters α , β , γ , and δ were obtained by fitting the H atom temporal profiles to eq II. Examples of the measured H atom temporal profile and the fit of this data to eq II are shown in Figure 2. During the course of these measurements, $[H_2O_2]$ was kept constant and concentrations of H_2 and HD were varied. The obtained values of δ_{H_2} and δ_{HD} were plotted against $[H_2]$ and $[HD]$ to obtain, respectively, the bimolecular rate coefficients k_1 and k_2 .

Using the above procedure, the value of k_2 determined at 298 K was $k_2 = (5 \pm 1) \times 10^{-15} \text{ cm}^3 \text{ molecule}^{-1} \text{ s}^{-1}$. At temperatures other than 298 K, the δ_{HD} parameter was not determined at many HD concentrations, because very large amounts of HD would have been required for these experiments. However, δ_{H_2} was measured as a function of $[H_2]$ at various temperatures, and the obtained values of k_1 are listed in Table 1. In general, they agree with the values obtained by observing OH profiles. Determining rate coefficients from the temporal profile of a product, by fitting to an eq such as eq II, is less precise than the values obtained by monitoring an exponential decay of a reactant. Therefore, we used only the data obtained by monitoring OH profiles for deriving the Arrhenius parameters reported in Table 2.

To determine the yield of H atoms in reaction 2, we carried out back-to-back experiments where HD was replaced with H_2 while maintaining all other parameters constant. The H atom resonance fluorescence signals were normalized for small changes in the resonance lamp output by using the background signal obtained before generating OH radicals. The signal for a given concentration of H atoms did not change significantly with H_2 concentration ($< 5\%$ decrease for doubling $[H_2]$). Because comparable concentrations of H_2 and HD were used, it was assumed that H atom detection sensitivity was the same in the two back-to-back experiments where HD was replaced by H_2 . By assuming that $[H_2O_2]$, laser fluence, k_{OH} , and detection sensitivity of H atom remained unchanged between the back-to-back experiments and by using eqs III and IV, we

TABLE 3: Branching Ratio, k_{2a}/k_2 , in OH + HD Reaction

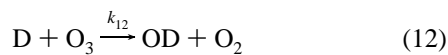
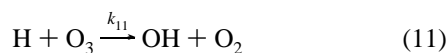
source of OH	temp (K)	branching ratio (k_{2a}/k_2)		
		measured	estimated from	
			k_1 and k_3	k_2 and k_3
H ₂ O ₂ /248 nm	250	0.17 ± 0.03	0.15	0.17
	298	0.28 ± 0.05	0.20	0.21
O ₃ /248 nm/H ₂ (HD)	298	0.24 ± 0.03	0.20	0.21

obtain the following expression for the branching ratio:

$$\frac{k_{2a}}{k_2} = \frac{\alpha_{\text{HD}}}{\alpha_{\text{H}_2}} \times \frac{k_1[\text{H}_2]}{k_2[\text{HD}]} \times \frac{\delta_{\text{HD}} - \beta_{\text{HD}}}{\delta_{\text{H}_2} - \beta_{\text{H}_2}} \quad (\text{V})$$

All parameters on the right-hand side of eq V can be obtained from the biexponential fits (eq II), the derived values of k_1 and k_2 , and the known concentrations of H₂ and D₂. Alternatively, the $k_1[\text{H}_2]$ and $k_2[\text{HD}]$ values can be obtained from the differences in the δ parameters measured with H₂ and HD and the intercepts of plots of δ_{H_2} vs [H₂] and δ_{HD} vs [HD]. Since only a limited number of HD concentrations were used and since the values of k_1 and k_2 measured by observing OH temporal profiles are more accurate, we used the computed values of $k_1[\text{H}_2]$ and $k_2[\text{HD}]$. The intercept of a plot of δ vs [H₂] or [HD] is $\delta_{\text{int}} = k_7[\text{H}_2\text{O}_2] + k_{\text{OH}}$. The measured values of δ_{int} in back-to-back experiments involving H₂ and HD were, within the experimental uncertainty, the same. This constancy showed that the concentration of H₂O₂ and, hence, [OH]₀, did not change during these experiments. The obtained values of the branching ratio are shown in Table 3 as the mean of a large number of back-to-back measurements. The quoted error bars are the standard deviation of the mean.

In a second series of experiments at 298 K, a small amount of O₃ ($<5 \times 10^{12} \text{ cm}^{-3}$) was photolyzed to generate O(¹D) in the presence of a large concentration of HD ($\sim 1 \times 10^{18} \text{ cm}^{-3}$). O(¹D) reacted with HD to make OH and OD. The sum of the concentration of OH and OD was equal to the initial concentration of O(¹D) that reacted with HD. The concentration of O₃ was small enough to prevent any significant loss of H or D atoms via the reactions



and subsequent H atom production via reactions of OH and OD with HD, even though k_{11} and k_{12} are rapid,¹³ $\sim 3 \times 10^{-11} \text{ cm}^3 \text{ molecule}^{-1} \text{ s}^{-1}$. The rate coefficients for the reaction of HD with OD should be equal to k_2 , and the branching ratio for H atom production in the two reactions should also be the same. Hence, the concentration of H atoms produced will depend on the sum of the concentrations of OH and OD. There was an instantaneous production of H atoms via the reaction of O(¹D) with HD. Following this jump, there was a slower production of H atoms via the reactions of OD and OH with HD. The temporal profiles of H atom were again fit to a biexponential expression, which was essentially the same as eq II with the exception that it included a term for the initial H atom produced by the O(¹D) + HD reaction. By comparing the signal due to the reaction of OD/OH with HD to that due to the reaction of O(¹D) with HD, the H atom yield was calculated. This method requires knowledge of the fractional yield of H atom in the O(¹D) + HD reaction, which was independently measured¹⁸ to be 0.57 ± 0.03 , in agreement with previously reported values.^{19–22} The obtained value of k_{2a}/k_2 is also listed in Table 3. The

branching ratios determined using the two different methods are in excellent agreement.

Discussion

The major sources of error in our measured values of k_1 – k_5 are the uncertainties in the concentrations of H₂, HD, or D₂, which are conservatively estimated to be 5% at the 95% confidence level, and the presence of reactive impurities. The latter possibility is important because k_1 – k_5 are small and, hence, very small amounts of impurities can lead to large errors. We have already mentioned that the level of impurities in H₂ and D₂ samples was too small to affect the measured values of k_1 and k_3 . Our purified sample of HD contained <10 ppmv of small hydrocarbons (CH₄ and C₂H₆). Even if we assume this impurity to be all C₂H₆, it would contribute less than 0.1% to the measured rate coefficient even at 245 K, the lowest temperature of our measurements. Since the same gas handling procedures were employed at different temperatures, systematic errors in the concentrations of the excess reagent, i.e., H₂, D₂, or HD, are the same at all the temperatures. Therefore, the uncertainties in E/R values shown in Table 2 are primarily determined by the measured temperature and the precision of k_1 – k_3 . The A factors, of course, are affected by the uncertainties in measuring concentrations of H₂, HD, and D₂.

Table 2 lists the parameters obtained by fitting our data to Arrhenius expressions and three-parameter forms, $k = AT^n e^{-E/RT}$. Such parameters from previous studies are also shown in the table. The average value of k_1 (298 K) measured here, $(6.65 \pm 0.36) \times 10^{-15} \text{ cm}^3 \text{ molecule}^{-1} \text{ s}^{-1}$, is in excellent agreement with the current recommendations.^{13,14} The quoted error bar includes an estimated systematic uncertainty of 5% in measuring the concentration of H₂ and 2σ precision in k_1 obtained from the fits of k' vs [H₂] data to a straight line. The Arrhenius parameters from our data are in excellent agreement with the recommendations.^{13,14} Oldenberg *et al.*²³ measured k_1 in the temperature range 800–1500 K. They combined their data with those of Ravishankara *et al.*,²⁴ Tully *et al.*,²⁵ Michael and Sutherland,²⁶ Frank and Just,²⁷ and Davidson *et al.*²⁸ and derived the expression $k_1 = 3.56 \times 10^{-16} T^{1.52} \exp[-1736/T] \text{ cm}^3 \text{ molecule}^{-1} \text{ s}^{-1}$, to cover 250–2581 K. This fit agrees well with our measured values, except at temperatures less than ~ 250 K, where it deviates by $\sim 20\%$.

The k_3 values between 250 and 1050 K reported by Ravishankara *et al.*²⁴ are in excellent agreement with those from the present study in the overlapping temperature range. The data of Smith and Zellner²⁹ appear to be systematically higher than those measured here and of Ravishankara *et al.* Nevertheless, the three sets of data agree within the combined error limits. We have combined Ravishankara *et al.*'s data with those from the present study to extract the recommended values of k_3 (298 K) and its temperature dependence, which are also shown in Table 2.

To check for a secondary isotope effect, we measured the rate coefficients for reactions 4 and 5. The 297 K value of k_5 measured by Paraskevopoulos and Nip³⁰ is 35% higher than our value at 298 K. Their measured value of k_3 is also $\sim 30\%$ higher than that measured here and by Ravishankara *et al.* The difference is likely due to the presence of impurities in the D₂ sample used by Paraskevopoulos and Nip. Our previously reported value³¹ of $(1.88 \pm 0.30) \times 10^{-15} \text{ cm}^3 \text{ molecule}^{-1} \text{ s}^{-1}$ at 298 ± 2 K is in good agreement with the present measurements. Because of the greater care taken here to analyze the samples, the present value supersedes our previously reported³¹ rate coefficient. Our observation that $k_4 = k_1$ and $k_5 = k_3$ shows the minimal amount of secondary kinetic isotope effect in the

reaction of hydroxyl radical with hydrogen. This is to be expected because the H or D atom in the hydroxyl group is merely a spectator and the mass difference between OH and OD is very small. Of course, this finding is consistent with theoretical calculations.^{1, 6}

There are no previous absolute measurements of k_2 . Ehhalt *et al.*³² measured k_1/k_2 at 298 K to be 1.65 ± 0.05 using a relative rate technique. The ratio of our measured k_1 and k_2 at 298 K yields $k_1/k_2 = 1.68 \pm 0.11$, if we assume that the systematic errors in our measurements of k_1 and k_2 are the same. The agreement between these two studies is excellent. The activation energy for reaction 2 is closer to that for reaction 1 than for reaction 3. This is to be expected if H atom abstraction is the major channel in reaction 2 (see below).

Table 3 shows the branching ratio, k_{2a}/k_2 , measured at 298 and 250 K. The ratio was measured at 298 K using two very different methods, and the values were found to agree with each other; this agreement enhances our confidence in this value. It can be easily shown that secondary reactions are not significant in our system. Attempts to measure this branching ratio at higher temperatures were not successful; they yielded inconsistent values and were not pursued further. The low H atom yield is consistent with a large fraction of reaction 2 proceeding via H atom abstraction.

To a zeroth order approximation, a reaction with a barrier such as that between OH and H₂ can be roughly divided into three energy regimes: (1) reactions at energies much higher than the barrier, where dynamical effects are dominant; (2) reactions at energies comparable to the barrier height, where the rate coefficients are sensitive to the height of the barrier; and (3) reactions at energies where passing over the barrier is essentially impossible and, hence, tunneling through the barrier is the most likely pathway. The third regime is particularly important for H atom transfer processes, such as the reaction under consideration here. Usually, dynamical calculations address the first two regimes, where the height of the barrier is of major importance. It appears that our data mostly refer to the third regime, where the width/shape of the barrier is likely to play a major role.

A large number of investigators have calculated the thermal rate constants for reactions 1 and 3 with varying degrees of agreement with measured values (see Clary⁵ and references therein). Most of these calculations are based on the *ab initio* PES of Walch and Dunning.³ Recently, Fisher and Michael³³ used the PES of Kraka and Dunning, which is believed to be better than the Walch and Dunning surface, to calculate k_1 and k_3 using transition state theory. They obtained remarkably good agreement between experimental data and their calculations over a very wide range of temperatures, 250–2500 K. Because rate coefficients in the temperature range ~500–2500 K are sensitive to the height of the barrier, Fisher and Michael could estimate this parameter well. In all these calculations, except the “exact quantum” methodologies,^{6,34–36} tunneling through the barrier was added *a posteriori* using a correction, such as the Wigner correction (see, e.g., ref 1). Therefore, comparison of our low-temperature data with theoretical calculations is not a very good test of the PES or the dynamics.

The reaction of OH with H₂ has been extensively studied theoretically as a “prototype” for quantum scattering calculations. Absolute rate coefficients, as well as kinetic isotope effects, have been calculated (see, e.g., Clary⁵) with varying levels of agreement between calculations and between calculations and experiments.

Zhang and Zhang,³⁶ in their time dependent quantum mechanical calculations of the reaction probabilities for the two

channels (reactions 2a and 2b) in the OH + HD reaction, attributed the low branching ratios for H atom production at low collision energies (below threshold) to the preferential tunneling of H over D atoms. The lowest collision energy used in their calculations, 2.8 kcal/mol, is much higher than the average collision energy in the temperature range of our experiments. The calculations of Zhang and Zhang³⁶ are qualitatively consistent with our results. Calculation of the thermal rate constants from reactive cross sections would be useful. Calculation of low-temperature rate constants requires cross sections at low collision energies, which are not always available.

In Figure 1, we compare the measured values of k_2 with those calculated by assuming them to be equal to half the sum of k_1 and k_3 . The agreement over the entire temperature range is amazing! With the same assumption, we can calculate the branching ratios for H atom production at different temperatures, which are also shown in Table 3. Again the agreement between the measured and the calculated values is excellent. These two observations suggest that when OH reacts with hydrogen, the identity of the uninvolved atom does not matter. If OH approaches an H atom, it abstracts the H atom as efficiently from H₂ as from HD. If it approaches the D atom of HD, it abstracts it with the same efficiency as from D₂. The OH + H₂ reaction is not a heavy–light–heavy system of the A + B–C type reaction. Yet it appears to behave as one! One simple (simplistic?) explanation for these observations is that the majority of the reaction proceeds via tunneling, as suggested by the calculations noted above. Measurements of k_1 , k_2 , k_3 , and k_{2a}/k_2 at much lower temperatures would be very useful to find out the cause(s) for our observations. However, such measurements are difficult to make. In the interim, our measured values of k_1 – k_3 should provide a consistent data set for testing the theoretical calculations.

Atmospheric Implications. The tropospheric lifetimes of HD, τ_{HD} , and H₂, τ_{H_2} , due to reaction with OH can be estimated using the formulation of Prather and Spivakovsky³⁷ by using the expression

$$\frac{\tau_{HD} \text{ or } \tau_{H_2}}{\tau_{CH_3CCl_3}} = \frac{k_{CH_3CCl_3}^{277 K}}{k_{HD}^{277 K} \text{ or } k_{H_2}^{277 K}} \quad (VI)$$

where $k_{CH_3CCl_3}^{277 K}$ is the rate coefficient for the reaction of OH with CH₃CCl₃ at 277 K, the weighted average temperature of the troposphere for removal of species via reaction with OH. $k_{HD}^{277 K}$ and $k_{H_2}^{277 K}$ are the rate constants at 277 K for the reactions of OH with HD and H₂, respectively. Using the tropospheric lifetime of CH₃CCl₃ due to reaction with OH, $\tau_{CH_3CCl_3}$, of 4.9 years,³⁸ we obtain tropospheric lifetimes for removal via OH for HD and H₂ of 14.5 and 8.5 years, respectively. Equation VI is a good approximation because hydrogen and CH₃CCl₃ are both well mixed and activation energies for the OH + CH₃CCl₃ and OH + H₂/HD reactions are not too different. In the above analysis, we assumed that the only loss process for H₂ and HD is reaction with OH in the troposphere. The atmospheric lifetimes of H₂ and HD would be ~8 and 14 years when stratospheric removal of these compounds is considered. Again, we are assuming that the only loss process for these two species in the stratosphere is via reaction with OH.

There would be a large isotopic fractionation if the primary loss of atmospheric hydrogen is due to its reaction with OH. Microbial uptake of hydrogen by soil is known to be isotope nonselective.³² However, if the microbial uptake is a major loss process for hydrogen, the ratio of HD/H₂ in the atmosphere

will be much smaller than that seen in the absence of a soil sink. Therefore, measurement of HD/H₂ ratios in the atmosphere and estimation of its sources can place limits on the microbial sink. Measuring the D/H ratio in atmospheric molecular hydrogen in conjunction with the measured values of k_1 and k_2 and the isotopic abundances of CH₃D is likely to help constrain the methane budget.

Acknowledgment. This work was funded in part by NOAA's Climate and Global Change Program and was carried out while Yinon Rudich held a National Research Council-NOAA Research Associateship and Leah Goldfarb held a NASA-Climate and Global Change Doctoral Fellowship. We are grateful to one of the reviewers for very insightful comments.

References and Notes

- (1) Michael, J. V. The measurement of thermal bimolecular rate constants by the flash photolysis-shock tube (FP-ST) technique: Comparison of experiment to theory. In *Advances in chemical kinetics and dynamics*; Barker, J. R., Ed.; JAI Press Inc.: Greenwich, CT, 1992; p 47.
- (2) Schatz, G. C.; Elgersma, H. *Chem. Phys. Lett.* **1980**, *73*, 21.
- (3) Walch, S. P.; Dunning, T. H., Jr. *J. Chem. Phys.* **1980**, *72*, 1303.
- (4) Dunning, T. H., Jr.; Harding, L. B.; Kraka, E. In *Supercomputer algorithms for reactivity, dynamics, and kinetics of small molecules*; Lagana, A., Ed.; Kluwer Academic Publishers: Dordrecht, The Netherlands, 1989; p 57.
- (5) Clary, D. C. *J. Phys. Chem.* **1994**, *98*, 10678.
- (6) Clary, D. C. *J. Chem. Phys.* **1992**, *96*, 3656.
- (7) Schatz, G. C.; Walch, S. P. *J. Chem. Phys.* **1980**, *72*, 776.
- (8) Talukdar, R. K.; Burkholder, J. B.; Schmoltner, A.-M.; Roberts, J. M.; Wilson, R.; Ravishankara, A. R. *J. Geophys. Res.* **1995**, *100*, 16.
- (9) Vaghjiani, G. L.; Ravishankara, A. R. *J. Phys. Chem.* **1989**, *93*, 1948.
- (10) Talukdar, R. K.; Warren, R. F.; Vaghjiani, G. L.; Ravishankara, A. R. *Int. J. Chem. Kinet.* **1992**, *24*, 973.
- (11) Talukdar, R.; Mellouki, A.; Gierczak, T.; Burkholder, J. B.; McKeen, S. A.; Ravishankara, A. R. *Science* **1991**, *252*, 693.
- (12) Warren, R. F.; Gierczak, T.; Ravishankara, A. R. *Chem. Phys. Lett.* **1991**, *183*, 403.
- (13) DeMore, W. B.; Sander, S. P.; Golden, D. M.; Hampson, R. F.; Kurylo, M. J.; Howard, C. J.; Ravishankara, A. R.; Kolb, C. E.; Molina,

- M. J. *Chemical Kinetics and Photochemical Data for use in Stratospheric Modeling*; JPL publication 94-26; Jet Propulsion Laboratory: 1994.
- (14) Atkinson, R.; Baulch, D. L.; Cox, R. A.; Hampson, R. F.; Kerr, J. A.; Troe, J. *J. Phys. Chem. Ref. Data* **1992**, *21*, 1125.
 - (15) Michael, J. V. *J. Chem. Phys.* **1990**, *92*, 3394.
 - (16) Michael, J. V.; Fisher, J. R. *J. Phys. Chem.* **1990**, *94*, 3318.
 - (17) Benson, S. W. *Thermochemical Kinetics*; John Wiley and Sons Inc.: New York, 1976; p 292.
 - (18) Talukdar, R. K.; Ravishankara, A. R. *Chem. Phys. Lett.*, in press.
 - (19) Matsumi, Y.; Tonokura, K.; Kawasaki, M.; Kim, H. L. *J. Phys. Chem.* **1992**, *96*, 10622.
 - (20) Tsukiyama, K.; Katz, B.; Bersohn, R. *J. Chem. Phys.* **1985**, *83*, 2889.
 - (21) Satyapal, S.; Park, J.; Bersohn, R.; Katz, B. *J. Chem. Phys.* **1989**, *91*, 6873.
 - (22) Laurent, T.; Naik, P. D.; Volpp, H.-R.; Wolfrum, J.; Arusi-Parpar, T.; Bar, I.; Rosenwaks, S. *Chem. Phys. Lett.* **1995**, *236*, 343.
 - (23) Oldenberg, R. C.; Loge, G. W.; Harradine, D. M.; Winn, K. R. *J. Phys. Chem.* **1992**, *96*, 8426.
 - (24) Ravishankara, A. R.; Nicovich, J. M.; Thompson, R. L.; Tully, F. P. *J. Phys. Chem.* **1981**, *85*, 2498.
 - (25) Tully, F. P.; Ravishankara, A. R. *J. Phys. Chem.* **1980**, *84*, 3126.
 - (26) Michael, J. V.; Sutherland, J. W. *J. Phys. Chem.* **1988**, *92*, 3853.
 - (27) Frank, P.; Just, T. *Ber. Bunsen-Ges. Phys. Chem.* **1985**, *89*, 181.
 - (28) Davidson, D. F.; Chang, A. Y.; Hanson, R. K. *Proc. Int. Symp. Combust.* **1988**, 1877.
 - (29) Smith, I. W. M.; Zellner, R. *J. Chem. Soc., Faraday Trans. 2* **1974**, *70*, 1045.
 - (30) Paraskevopoulos, G.; Nip, W. S. *Can. J. Chem.* **1980**, *58*, 2146.
 - (31) Vaghjiani, G. L.; Ravishankara, A. R.; Cohen, N. *J. Phys. Chem.* **1989**, *93*, 7833.
 - (32) Ehhalt, D. H.; Davidson, J. A.; Cantrell, C. A.; Friedman, I.; Tyler, S. *J. Geophys. Res.* **1989**, *94*, 9831.
 - (33) Fisher, J. R.; Michael, J. V. *J. Phys. Chem.* **1990**, *94*, 2465.
 - (34) Clary, D. C. *J. Chem. Phys.* **1991**, *95*, 7298.
 - (35) Zhang, D. H.; Zhang, J. Z. H. *J. Chem. Phys.* **1994**, *101*, 1146.
 - (36) Zhang, D. H.; Zhang, J. Z. H. *Chem. Phys. Lett.* **1995**, *232*, 370.
 - (37) Prather, M.; Spivakovsky, C. M. *J. Geophys. Res.* **1990**, *95*, 18723.
 - (38) Prinn, R. G.; Weiss, R. F.; Miller, B. R.; Huang, J.; Alyea, F. N.; Cunnold, D. M.; Fraser, P. J.; Hartley, D. E.; Simmonds, P. G. *Science* **1995**, *269*, 187.
 - (39) Stuhl, F.; Niki, H. *J. Chem. Phys.* **1972**, *57*, 3671.
 - (40) Greiner, N. R. *J. Chem. Phys.* **1968**, *48*, 1413.

JP9518724